Chem. Mater. **1997,** 9, 119−126

Pulsed Laser Deposition of $Ba_{2-x}A_xCuO_2CO_3$ (A = Ca, Sr) Thin Films, $m = 0$ Member of the Series $(CaCuO_2)_m(Ba_{2-x}A_xCuO_2CO_3)_n$ (A = Ca, Sr)

W. Prellier,[*,†] A. Tebano,[‡] J. L. Allen,[†] J. F. Hamet,[†] B. Mercey,[†]
M. Hervieu,[†] and B. Raveau[†]

Laboratoire CRISMAT, ISMRA et Université de Caen, 6 Bd du Maréchal Juin,
14050 Caen Cedex, France, and INFM, Dipartimento di Ingegneria Meccanica,
Universitá di Roma 'Tor Vergata', Via della Ricerca Scientifica, 00133, Roma, Italy

Received April 25, 1996. Revised Manuscript Received September 10, 1996[⊗]

Copper oxycarbonate thin films of the $(CaCuO_2)_m(Ba_{2-x}A_xCuO_2CO_3)_n$ (A = Ca, Sr) system have been deposited, using the pulsed laser deposition (PLD) technique, on (100) $LaAlO_3$ and (110) $NdGaO_3$ substrates. The $m = 0$ member of the family, $Ba_{2-x}Sr_xCuO_2CO_3$ ($x = 0.1$ and $x = 0.4$) has been deposited in a selective way for the first time on both $LaAlO_3$ and $NdGaO_3$. The best results have been obtained for $NdGaO_3$ substrates, but a double orientation of the film, [001] and [110], is found by transmission electron microscopy (TEM) for $x = 0.4$. $Ba_{2-x}Ca_xCuO_2CO_3$ ($x = 0.2$) has also been studied. At a deposition temperature of 620 °C, a $Ba_2CuO_2CO_3$ (B_2CC) type structure is stabilized, whereas at 680 °C another perovskite is isolated. Attempts to deposit the member ($m = 1$, $n = 1$, $x = 0$) of the family, i.e., $Ba_2CaCu_2O_4CO_3$, on $LaAlO_3$ using a single multiphase sintered ceramic target led to the formation of a B_2CC type structure ($m = 0$) coherently intergrown with $CaCu_2O_3$ and Ca_2CuO_3 extended defects. The structures and structural mechanisms are discussed. No diamagnetic transition was observed in any of these films down to 5 K.

1. Introduction

Nine years after the discovery of $YBa_2Cu_3O_{7-\delta}$, many cuprate compounds have been found to exhibit superconductivity. Typically, bulk synthetic techniques have been used for this search. Recently, high-pressure methods[1−3] and thin-film growth, by pulsed laser deposition particularly,[4,5] have been shown to offer possibilities for synthesizing new metastable phases.

Progress in the understanding of the epitaxial thin film growth of cuprates has heightened interest in creating artificially layered structures.[6,7] The layered structures of the cuprate superconductors open the way to new materials if one can control carefully each layer. The recent discovery of the oxycarbonate thin-film superconductor $(CaCuO_2)_m(Ba_2CuO_2CO_3)_n$[8,9] is of great interest owing to its critical temperature $T_{c(\mathrm{offset})} = 75$ K, $T_{c(\mathrm{onset})} = 110$ K that makes this material a serious competitor for $YBa_2Cu_3O_7$. The structure of these oxycarbonates consists of "infinite layer"-type structure, ($m - 1$) copper layers thick, interconnected through layers of carbonate groups sandwiched between two pyramidal copper layers. For example, the idealized structural model of the first member of the family, $m = 1$, $n = 1$, i.e., $Ba_2CaCu_2O_4CO_3$ is shown in Figure 1. Such superconducting films were prepared using a $Ba_2Ca_3Cu_4O_x$ target on $LaAlO_3$ as substrate. The average m value corresponds to the nominal one, that is m

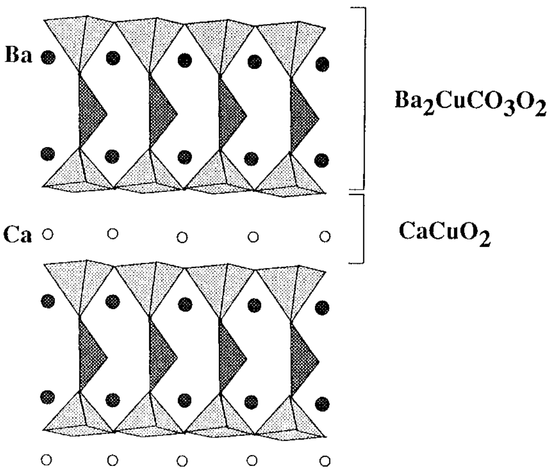

Figure 1. Idealized drawing of the structure $(CaCuO_2)_1(Ba_2CuCO_3O_2)_1$.

[†] Laboratoire CRISMAT.

[‡] INFM.

[⊗] Abstract published in *Advance ACS Abstracts,* November 15, 1996.

(1) Jin, C. Q.; Wu, X. J.; Laffez, P.; Taksuki, T.; Tamura, T.; Adachi, S.; Yamauchi, H.; Kashizuka, N.; Tanaka, T. *Nature* **1995**, *375*, 301.

(2) Hiroi, Z.; Takano, M. *Physica C* **1994**, *235*−240, 29.

(3) Alario-Franco, M. A.; Bordet, P.; Capponi, J. J.; Chaillout, C.; Chenavas, J.; Tournier, T.; Marezio, M.; Souletie, B.; Sulpice, A.; Tholence, J. L.; Colliex, C.; Argoud, R.; Baldonedo, J. L.; Gorius, M. F.; Perroux, M. *Physica C* **1994**, *231*, 103.

(4) Allen, J. L.; Mercey, B.; Hervieu, M.; Hamet, J. F.; Raveau, B. *J. Mater. Chem.* **1996**, *6*, 1141.

(5) Niu, C.; Lieber, C. *Appl. Phys.* **1994**, *L61*, 1712.

(6) Matunari, S.; Kanai, M.; Kawai, T. *Jpn. J. Appl. Phys.* **1994**, *L20*, 34.

(7) Norton, D. P.; Chakoumakos, B. C.; Budai, J. D.; Lowdes, D. H.; Sales, B. C.; Thompson, J. R. Christen, D. K. *Science* **1994**, *265*, 2074.

(8) Allen, J. L.; Mercey, B.; Prellier, W.; Hamet, J. F.; Hervieu, M.; Raveau, B. *Physica C* **1995**, *241*, 158.

(9) Hervieu, M.; Mercey, B.; Prellier, W.; Allen, J. L.; Hamet, J. F.; Raveau, B. *J. Mater. Chem.* **1996**, *6*, 165.

S0897-4756(96)00250-5 CCC: $14.00

= 3,[8] but the high-resolution electron microscopy study shows that different members with a variable number of $CaCuO_2$ units usually coexist.[9]

Thus, considering the above results, it is of prime importance to grow single-phase thin films of each member of the series in order to reach the highest $T_{c(\mathrm{offset})}$ which should be close to 110 K. Using a multitarget system, our aim is to stabilize "layer by layer" each member of the series. The simplest system would be to consider $Ba_2CuCO_3O_2$ and $CaCuO_2$ targets. For such a goal, we need to understand the way the parent structures behave when they are deposited as a thin film. This paper deals with the growth and the characterization of thin films deposited for nominal compositions $Ba_{2-x}A_xCuO_2CO_3$ ($n = 1$, $m = 0$, A = Ca, Sr) and $Ba_2CaCu_2O_4CO_3$ ($n = 1$, $m = 1$).

2. Experimental Section

Five targets of nominal composition $Ba_2CaCu_2O_x$, $Ba_{1.9}Sr_{0.1}CuO_x$, $Ba_{1.6}Sr_{0.4}CuO_x$, $Ba_{1.8}Ca_{0.2}CuO_x$, and $Ba_{1.5}Ca_{0.5}CuO_x$ were prepared by solid-state reaction. A well-ground mixture of $BaCO_3$, $SrCO_3$, $CaCO_3$, and CuO powders, weighed to the nominal composition of the target, was calcined at 650 °C for 10 h. After grinding, the resultant was fired at 800 °C, in air. The powders were ground again, pressed into a pellet, and sintered at 940 °C.

A pulsed KrF excimer laser (Lambda Physik LPX200, $\lambda = 248$ nm) was used for film deposition. The substrates are (100) $LaAlO_3$ and (110) $NdGaO_3$. The crystallographic structure of $LaAlO_3$ is pseudocubic ($a = 3.788$ Å) and $NdGaO_3$ is orthorhombic with $a = 5.426$ Å, $b = 5.502$ Å, and $c = 7.706$ Å. The details of the geometry of the experiment have been previously described.[4] Briefly, a rotating target producing a plume of ablated material perpendicular to the substrate placed at a distance around 5 cm. The beam, directed into the deposition chamber with an angle of 45°, is focused on the target with a fluence of 2 J/cm^2, and the rate is 4 Hz. The heater was kept at a constant temperature ranging from 600 to 700 °C during deposition. A gas mixture of O_2 and CO_2 at a pressure around 0.2 mbar was used. After deposition, the samples were slowly cooled to room temperature with the same gas composition at a pressure of 500 mbar. The total number of pulses used throughout the deposition was 7000 with a deposition rate around 0.4 Å/pulse for each material; the typical thickness of a film was about 3000 Å.

The structural study was carried out by X-ray diffraction using a Seifert XRD 300 diffractometer with Cu Kα_1 radiation ($\lambda = 1.5405$ Å) for the $\theta-2\theta$ measurements. The step used was 0.02° with a counting time of 1 s. The levelness of the film was checked by adjusting the position of the two most intense diffraction peaks of the substrate by a rocking curve. The error in the interplanar distance was around 0.01 Å. Transmission electron microscopy (TEM) was performed with a JEOL 200 CX microscope and high-resolution electron microscopy (HREM) with a TOPCON 002B, having a point resolution of 1.8 Å. Errors on the cells dimensions, deduced from the electron diffraction data, are around 5%. Each microscope is equipped with an energy-dispersive scattering (EDS) analyzer.

3. Results and Discussion

To stabilize "layer by layer" the different members of the series, using a multitarget system, our first approach was to use two separate targets: $Ba_2CuO_2CO_3$ and $CaCuO_2$. The film could then be grown by alternate ablation from one target to another with a predetermined number of laser pulses. In this case, the layer thickness is controlled by counting laser pulses.

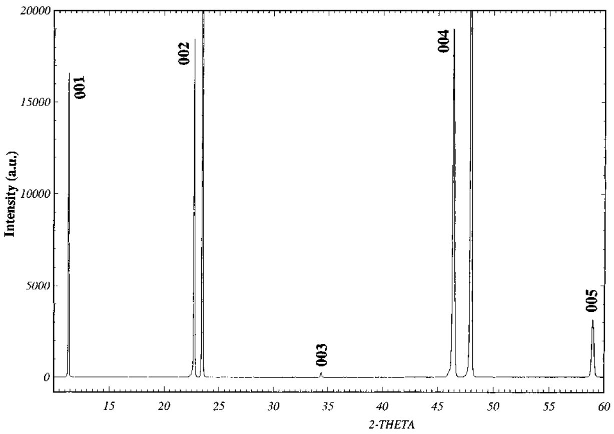

Figure 2. XRD diffractogram of $Ba_{1.6}Sr_{0.4}CuO_2CO_3$ on $LaAlO_3$.

Unfortunately, the $m = 0$ oxycarbonate member we wanted to stabilize, i.e., $Ba_2CuCO_3O_2$, was not stable unlike $Sr_2CuCO_3O_2$. Therefore, in a second step, we attempted to stabilize the $m = 0$ member by partly substituting Sr or Ca for Ba with the aim of synthesizing a member with a composition close to $Ba_2CuO_2CO_3$.

3.1. Member $m = 0$: $Ba_{2-x}A_xCuO_2CO_3$ (A = Sr and Ca). (i) $Ba_{2-x}Sr_xCuO_2CO_3$ ($x = 0.1$ and $x = 0.4$). Two targets with the nominal composition $Ba_{1.9}Sr_{0.1}CuO_x$ and $Ba_{1.6}Sr_{0.4}CuO_x$ were made. Primary attempts were made on $LaAlO_3$. As an example, the XRD pattern of the $Ba_{1.6}Sr_{0.4}CuO_2CO_3$ film is shown in Figure 2. XRD showed that the periodicity along the c axis, normal to the substrate, is 7.8 Å. Such a value is consistent with that expected for the $m = 0$ member[10] and suggests that the film is c axis oriented. The ED study indicates textured but not epitaxial films. This substrate effect is not surprising, and it confirms the prominent role of the substrate. Similar results have been obtained during the stabilization of other metastable phases such as the infinite layer cuprate $Ca_{1-x}Sr_xCuO_2$.[11]

Changing the substrate from $LaAlO_3$ to $NdGaO_3$ results in similar X-ray diffraction. XRD patterns of $Ba_{1.9}Sr_{0.1}CuO_2CO_3$ and $Ba_{1.6}Sr_{0.4}CuO_2CO_3$, grown on $NdGaO_3$, are displayed in Figure 3a,b. From XRD, the lattice parameter is calculated to be 7.9 Å for $x = 0.1$ and 7.8 Å for $x = 0.4$, which is in agreement with a partial substitution of Ba by Sr. These values can be compared to the c parameter obtained for the $x = 0.44$ bulk material which exhibits a tetragonal cell $a = 5.56$ Å and $c = 7.85$ Å.[12]

A microstructural study was carried out to clarify the film orientation. The EDS analyses performed for every film, on several zones of the film, show that the average cationic composition exactly correspond to the nominal composition of the target. The ED pattern taken along the direction perpendicular to the substrate is shown in Figure 4a. The intense reflections correspond to a simple cubic perovskite but extra reflections are observed. The extra spots belong to three systems which are systematically superimposed: the first system corresponds to extra spots at $^1/_2$ $^1/_2$ 0 positions, the second

---

(10) Armstrong, A. R.; Obhi, H. S.; Edwards, P. P. *J. Solid State Chem.* **1993**, *106*, 120.

(11) Balestrino, G.; Desfeux, R.; Martelucci, S.; Paoletti, A.; Petrocelli, G.; Tebano, A.; Mercey, B.; Hervieu, M. *J. Mater. Chem.* **1995**, *5*, 1879.

(12) Izumi, F.; Kinoshita, K.; Matsui, Y.; Yanagisawa, K.; Ishigaki, T.; Kamiyama, T.; Yamada, T.; Asamo, H. *Physica C* **1992**, *196*, 227.

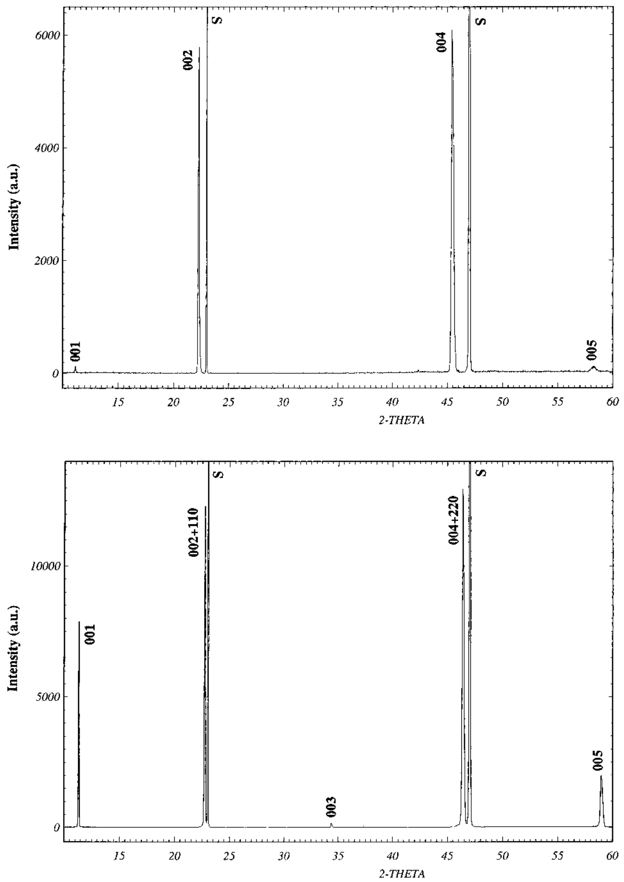

Figure 3. XRD diffractogram of (a, top) $Ba_{1.9}Sr_{0.1}CuO_2CO_3$ on $NdGaO_3$ and (b, bottom) $Ba_{1.6}Sr_{0.4}CuO_2CO_3$ on $NdGaO_3$ S indicates peaks of the substrate.

set at $^1/_2$ 0 0 positions, and the third one is similar to the second one but rotated by 90°. The reconstruction of the reciprocal space shows that the cell parameters are similar to those observed in the bulk material,[12] i.e., they involve a 4-fold cell with $a = b \approx \sqrt{2}a_p$, and $c \approx 2a_p$. In Figure 4a, the extra reflections of the three systems are indexed in the 4-fold cell. The different systems are denoted by subscripts 1, 2, and 3. These ED patterns reveal that the film is not only c axis oriented, as inferred from the XRD patterns. The second and third systems of extra spots show indeed that a part of the film is [**110**] oriented. The [**110**] oriented grains exhibit two possible orientations of the c axis, in-plane but perpendicular. The three grain orientations are schematically drawn in Figure 4b. Moreover, the rather perfect superposition of the three systems of extra spots shows that $d_{110} \approx d_{002}$. This explains why the different orientations are not detectable in the XRD data.

The sharpness of the reflections in the $\theta-2\theta$ scan attests to a good crystallinity of the film, which is confirmed by HREM. An example HREM image recorded along the direction perpendicular to the substrate is given in Figure 5a; the corresponding calculated images are displayed in Figure 5b. One clearly observes two domains. In the left part of the image (labeled **1**), the contrast consists of rows of very bright spots, 7.8 Å spaced, alternating with one row of smaller bright dots. This contrast fits well with that calculated for a [110] image (left part of Figure 5b) and is in agreement with the observations made in similar materials.[13,14] The rows of very bright dots are correlated to the carbonate rows and the smaller ones to the copper layers. In the right part of the image (labeled **2**), the contrast consists of a square array of bright dots, 5.4 Å spaced. Such an image corresponds to a [001] oriented domain. Along that direction, the copper and carbon atoms are projected over the same point, and the classical contrast of the perovskite-related compounds is observed. The calculated image is given in the right part of Figure 5b. This image shows that the junction (marked by an arrow and labeled B) between these two [001] and [110] domains is ensured without any stress. The structural model illustrates the way these two matrixes are connected (Figure 5c) and explains why such a junction (**B**) does not exhibit any stress. Owing to the Jahn–Teller effect of copper, the periodicity marked by the O–O distance[15] along c_2 (2.4 + 2 × 2.6 = 7.6 Å) in the domain **2** fits exactly with the double of the periodicity along $[110]_1$ (2 × 3.8 Å) in the domain **1**.

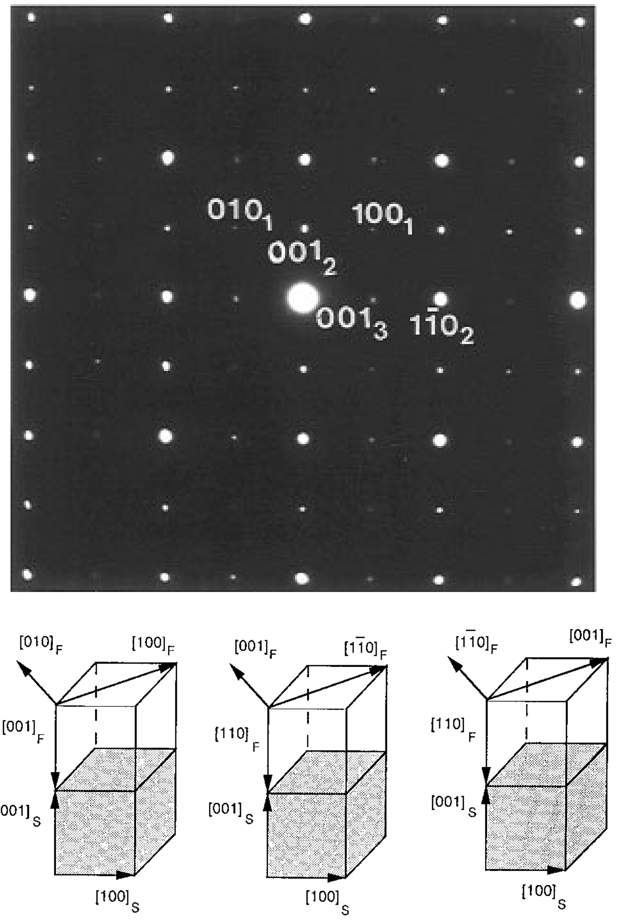

Figure 4. $Ba_{1.6}Sr_{0.4}CuO_2CO_3$: (a, top) ED taken along the direction perpendicular to the substrate and (b, bottom) schematic drawing of the three possible orientations of the grains. S refers to the substrate, and F refers to the film.

(ii) $Ba_{2-x}Ca_xCuO_2CO_3$ (x = 0.2). Two targets with nominal compositions $Ba_{2-x}Ca_xCuO_2CO_3$ (x = 0.2 and x = 0.5) were prepared by solid-state reaction. The substrate is (110) $NdGaO_3$. For x = 0.2, two deposition

---

(13) Y. Myazaki, Y.; Yamane, H.; Kajitani, T.; Oku, T.; Hiraga, K.; Morii, Y.; Fuchizaki, K.; Funahashi, S.; Hirai, T. *Physica C* **1992**, *196*, 434.

(14) Milat, O.; Van Tendeloo, G.; Amelinckx, s.; Babu, T. G. N.; Greaves, C. *J. Solid State Chem.* **1994**, *109*, 5.

(15) Nakata, H.; Akimitsu, J.; Katano, S.; Minami, T.; Ogita, N.; Udagawa, M.; *Physica C* **1995**, *255*, 157.

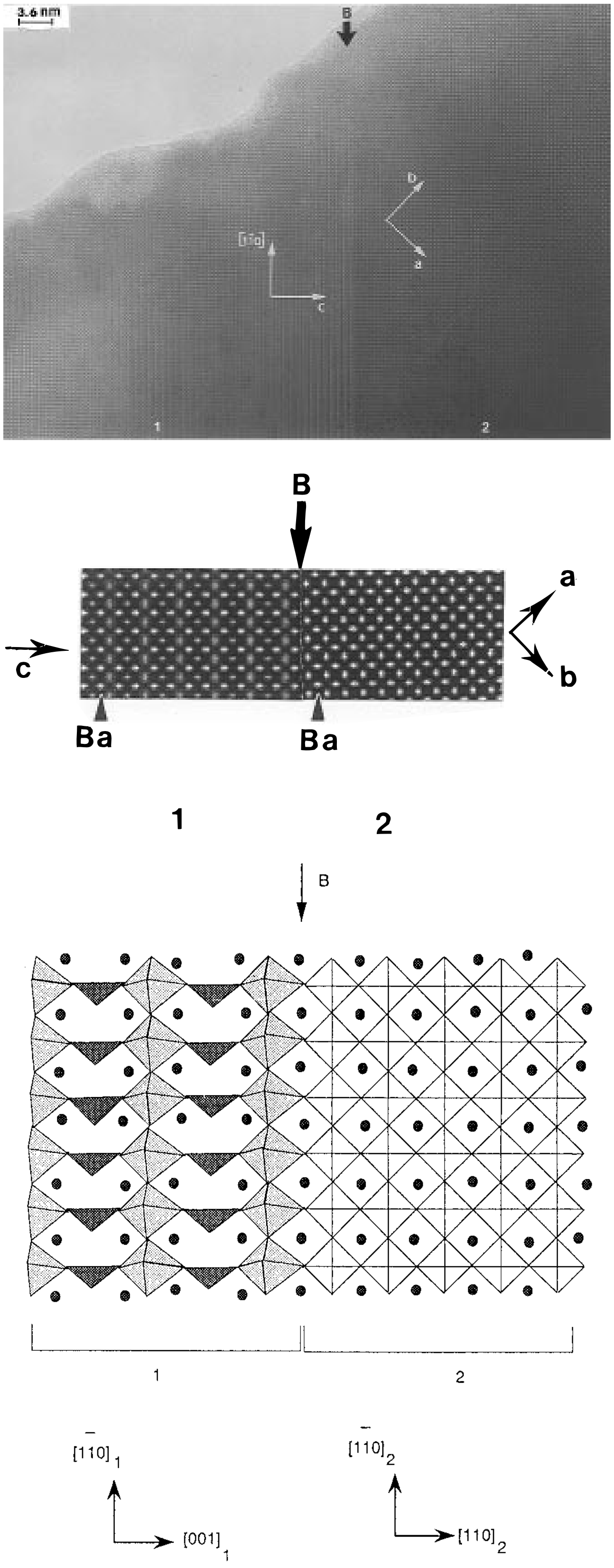

Figure 5. $Ba_{1.6}Sr_{0.4}CuO_2CO_3$: (a, top) HREM image of taken along a direction perpendicular to the substrate. Two domains are labeled **1** and **2**, separated by a planar boundary (B). (b, middle) Calculated images for the two domains (crystal thickness ≈25 Å and focus value −250 Å). The cation positions appear as dark dots (only barium positions are indicated). (c, bottom) Structural model illustrating the relative orientations of the two matrixes and the planar boundary.

temperatures were used for film deposition, 620 and 680 °C, but the other parameters of the thermal treatment were not modified.

From XRD patterns displayed in Figures 6, the lattice parameters perpendicular to the substrate plane are different for the two films corresponding to the same composition $x = 0.2$ but deposited at 620 and 680 °C. A c parameter close to 7.89 Å is observed for the film deposited at low temperature, whereas a c value close to 8.05 Å is observed at high temperature. The ED and HREM study shows that the two phases exhibit orthorhombic cells with $a \approx b \approx \sqrt{2}a_p$ and $c \approx 2a_p$ and both are c oriented. If the first c parameter, which corresponds to a small decrease of c with regard to the undoped $Ba_2CuO_2CO_3$ c parameter (7.89 Å instead of 7.97 Å) is in agreement with the Ca for Ba substitution the second (8.05 Å) is abnormal and suggests that a structural change occurred.

The low-temperature form corresponds to the expected one, i.e., $Ba_{1.8}Ca_{0.2}CuO_2CO_3$, and exhibits the B_2CC-type structure of the ($n = 1$, $m = 0$) member.

The high-temperature form is another perovskite-related form where two types of layers are observed along c: one layer where CuO_6 octahedra are partly replaced by CaO_6 octahedra and the second layer where CuO_6 octahedra and carbonate groups are located.[16] Note that the calcium and carbonate compositions seem to be ill defined in these materials. The $x = 0.2$ composition, namely, $Ba_{1.8}Ca_{0.2}CuO_2CO_3$, exhibits exactly the same Ba/Cu content as the $Ba_4CaCu_{2.25}(CO_3)_{0.75}O_y$ structure.[17] For $x = 0.5$, this second phase is deposited.

Two important points are highlighted by these results. First, they show that calcium can be partially substituted for barium and stabilized with the B_2CC-type structure. This mechanism is similar to that observed with strontium (above section); however, the solid solution is significantly more limited for calcium. This can be easily understood from ionic radii considerations. The difference between the size of Ca^{2+} and Ba^{2+} is too large to be adapted over a large range by the $[BaO_3]$ layers. When the calcium content is too high, calcium partly occupies the copper sites and the structure is stabilized by the presence of carbonates. The results observed for the $x = 0.2$ films show that temperature and CO_2 pressures are important parameters to stabilize one or the other phase.

3.2. Attempt to Synthesize $(CaCuO_2)(Ba_2CuCO_3O_2)$ ($m = 1$): Deposition of the $m = 0$ Member $Ba_{2-x}Ca_xCuO_2CO_3$. As mentioned above, $Ba_2CuO_2CO_3$ is not stable in air, but in fact this member can be stabilized by strontium for barium substitution. As a result, the deposition of the different members of the family, layer by layer, using a multitarget technique, would impose either to work with strontium or calcium doping and to study the series $(CaCuO_2)_m(Ba_{2-x}A_xCuCO_3O_2)_n$ (A = Ca, Sr) or to find another target in the place of $Ba_2CuO_2CO_3$.

Since it appears impossible to grow, as expected, the oxycarbonate films starting from $Ba_2CuO_2CO_3$ and $CaCuO_2$ targets, we chose to prepare the strontium-free members $(CaCuO_2)_m(Ba_2CuCO_3O_2)$, using a second tar-

---

[16] Kikuchi, M.; Ohshima, E.; Kikuchi, M.; Atou, T.; Syono, Y. *Physica C* **1994**, *223*, 263.

[17] Greaves, C.; Slater, P. R. *J. Mater. Chem.* **1991**, *1*, 17.

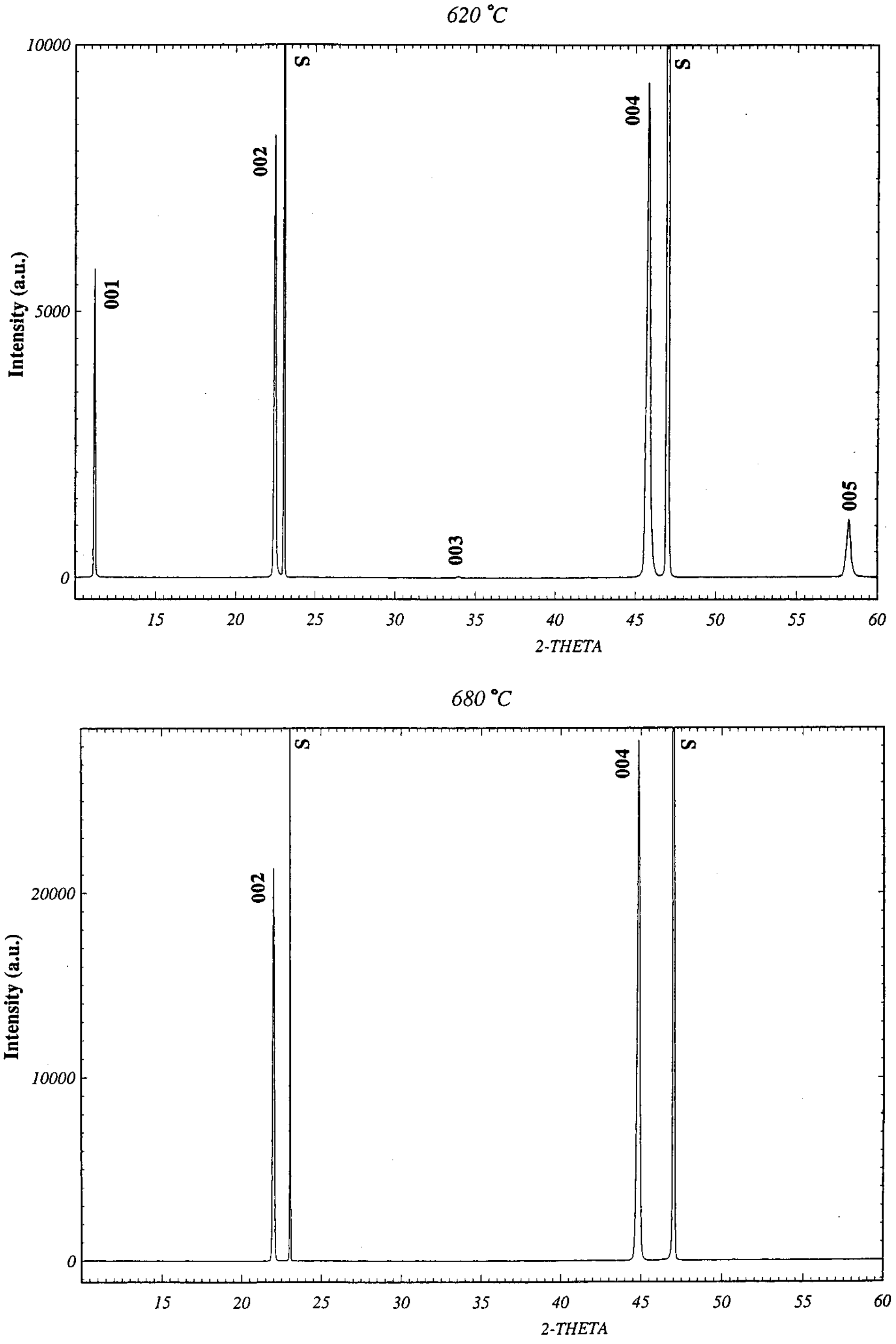

Figure 6. XRD diffractograms recorded for $Ba_{1.8}Ca_{0.2}CuO_2CO_3$ on $NdGaO_3$, deposited at low temperature (620 °C) and high temperature (680 °C). S indicates peaks of the substrate.

get of composition $Ba_2CaCu_2O_4CO_3$, i.e., that of the $n = 1$ and $m = 1$ member of the series. The other members will be then simply obtained by stacking the $m = 1$ and $n = 1$ member with $m - 1$ ($CaCuO_2$) layers. The first step of such a work is to study the structure deposited in these conditions. The results are presented hereafter.

The films were grown on $LaAlO_3$. A cap layer of $SrTiO_3$ deposited at room temperature was necessary to protect the film in air. Four peaks appear in the XRD pattern (Figure 7) at $2\theta = 11.37°$, 22.59°, 45.96°, and 58.56°. They correspond to a periodicity of 7.8 Å. Previous work on these oxycarbonates[9] showed that the cell parameters of the different members, characterized by m and n values, can be roughly estimated to $a \approx a_p$ and $c \approx 2 \times n \times a_p + 3.2 \times m$ Å. For the first member, $Ba_2CaCu_2O_4CO_3$, the c axis should be close to 11 Å. However, for this composition, another structure is deposited, which has been studied by ED and HREM.

The ED pattern (Figure 8a) recorded along the direction perpendicular to the substrate shows one single set of intense spots corresponding to a perovskite like structure with $a \approx b \approx a_p$, no condition limiting the reflections. However, an orthorhombic distortion and weak diffuse streaks, along [100]* and [010]*, are systematically observed. This suggests order–disorder phenomena take place in the matrix. The corresponding overall image is given in Figure 8b. The matrix exhibits

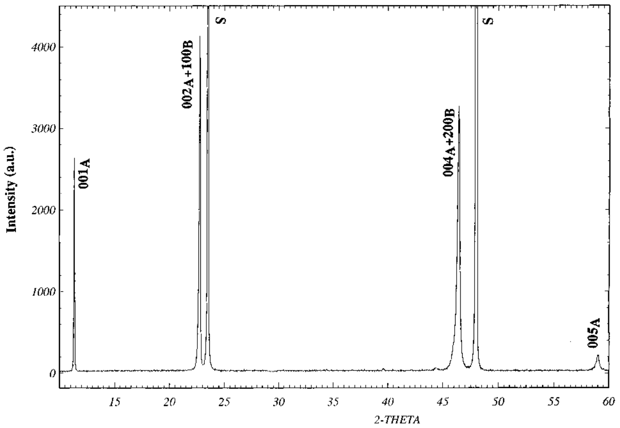

Figure 7. XRD diffractogram observed for the deposition of the composition $Ba_2CaCu_2O_4CO_3$. S indicates peaks of the substrate. A refers to the $Ba_{2-x}Ca_xCuCO_3O_2$ phase. B refers to the infinite layer $CaCuO_2$.

a contrast which consists of a square array of white spots at a spacing of 3.9 Å. This contrast would, in fact, be similar for every [001] oriented member of the family. The periodicity along the perpendicular direction and the reconstruction of the reciprocal space confirm the cell parameters $a \approx a_p \approx 3.9$ Å and $c \approx 2a_p \approx 7.8$ Å. These parameters correspond to those of the $m = 0$ member, $Ba_{2-x}Ca_xCuO_2CO_3$. The c parameter refined from XRD data, is significantly smaller than that of the calcium-free oxycarbonate, $Ba_2CuO_2CO_3$, 7.8 Å instead of 7.97 Å,[10] attesting that calcium partly replaces barium. The EDS analyses performed in several zones of the film show that the actual cationic composition of the film corresponds to Ba_2CaCu_2, i.e., in agreement with the nominal one $Ba_2CaCu_2O_4CO_3$. We can therefore consider that all the species have been transported during the deposition process. However, the HREM images (Figure 8b) show that numerous defects take place in the matrix so that the actual composition is only an average composition.

The defects appear as rectangular shaped domains, parallel to a or b. Some of these defects are marked by arrows in Figure 8b. An enlarged image of such a defect is given in Figure 9a. Inside the defective rectangle, the white spots are spaced by 3.9 Å in one direction and 3.2 Å in the perpendicular direction. This contrast is similar to that observed in the infinite layer structures[18] and to that observed in the oxycarbonates with high m values.[9] The rectangular defects consist of [010] $CaCuO_2$ domains in a [001] $Ba_2CuO_2CO_3$ matrix. The c_{cc} axis of the $CaCuO_2$ structure is parallel to the a_{B2CC} axis of the tetragonal mother structure $Ba_2CuO_2CO_3$. As in the $m = 3$ member of the oxycarbonate family, the $[CuO_2]_\infty$ layers of the $CaCuO_2$ domains are perpendicular to the substrate plane. The square-planar CuO_4 groups are systematically parallel to the length of the rectangle shaped $CaCuO_2$ domains. Along the width of the rectangular domains, the strong difference between the a_{B2CC} parameter (≈3.9 Å) and the c_{cc} parameter (≈3.2 Å) is accommodated through the formation of layers of different nature which run in the perpendicular direction (i.e., parallel to b_{cc} and b_{B2CC}). Two types of new layers are observed, they are indicated by white arrows in Figure 9a. In the right part of the image (arrow labeled R), one observes the formation of a double row of staggered bright dots, ≈2.3 Å spaced. It corresponds to the local formation of a rock salt-type layer, i.e., to the local formation of one Ca_2CuO_3 layer.[19] In the lower part of the defect (labeled P), there is a double row of gray dots, only ≈1.9 Å spaced. It corresponds to the local formation of a double copper layer, i.e., to the local formation of one $CaCu_2O_3$ layer.[20] Along the length of the rectangular domains, the difference between the b_{cc} and b_{B2CC} spacing is significantly smaller but exists. As a result, it locally causes the formation of interface dislocations. Two of them are indicated by curved arrows in Figure 9a. A schematic model of this defect can be proposed (Figure 9b).

The microstructure of the $Ba_2CaCu_2O_4CO_3$ film can therefore be described from the formation of a patchwork of [100]-oriented $CaCuO_2$ domains within a [001]-oriented $Ba_{2-x}Ca_xCuO_2CO_3$ matrix. The $m = 1$ member which would correspond to the regular intergrowth of one [100] $[CaCuO_2]_\infty$ layer with one [001] $[Ba_2CuO_2CO_3]_\infty$ layer has not been stabilized. The width of the $[CaCuO_2]$ domains rarely exceed six or seven layers.

It seems that the infinite layer structure $CaCuO_2$ is the dominant factor for the orientation, because the intercalation of additional $[CaCuO_2]_\infty$ layers, in the higher m members, forces the $Ba_2CuO_2CO_3$ to be a-axis oriented. If one indeed uses a single target of $Ba_2Ca_2Cu_3O_6CO_3$ or $Ba_2Ca_3Cu_4O_8CO_3$, the film is [100] oriented.[9] The fact that the c axis of the $CaCuO_2$ structure is parallel to the substrate plane may result from the low temperature of deposition, as seen in the case of $YBa_2Cu_3O_7$[21] or from the $LaAlO_3$ substrate.

4. Concluding Remarks

We have studied the primary stages of the growth of oxycarbonate cuprate thin films in the $(CaCuO_2)_m(Ba_{2-x}A_xCuCO_3O_2)_n$ (A = Ca, Sr) system using the pulsed laser deposition technique.

The first step was to stabilize the $m = 0$ member, $Ba_2CuCO_3O_2$, of the series. As this oxycarbonate is not stable in air, we propose an alternative solution to make this film by partially substituting Sr for Ba in the oxycarbonate and utilising a multitarget system. In this way, we have stabilized two oxycarbonates of the solid solution $Ba_{2-x}Sr_xCuO_2CO_3$, $x = 0.1$ and $x = 0.4$. $NdGaO_3$ was revealed as an interesting and useful substrate. However, a double orientation has been observed for the $x = 0.4$ film. After, we deposited $Ba_{2-x}Ca_xCuO_2CO_3$ ($x = 0.2, 0.5$). Moreover, the solid series is smaller than for $Ba_{2-x}Sr_xCuO_2CO_3$ as we get the B_2CC type structure only for small calcium content ($x = 0.2$) and at low deposition temperature (620 °C).

In a second step, we used another target corresponding to the member $m = 1$ coupled with a $CaCuO_2$ target to generate the higher member of the family. We have thus studied the microstructure of the strontium free, $m = 1$, $n = 1$ member, $Ba_2CaCu_2O_4CO_3$. The structure

---

(18) Mercey, B.; Gupta, A.; Hervieu, M.; Raveau, B. *J. Solid State. Chem.* **1995**, *116*, 37.

(19) Teske, C. L.; Müller-Buschbaum, H. K. *Z. Anorg. Allg. Chem. Mater.* **1994**, *371*, 325.

(20) Teske, C. L.; Müller-Buschbaum, H. K. *Z. Anorg. Allg. Chem. Mater.* **1969**, *370*, 134.

(21) Hamet, J. F.; Mercey, B.; Hervieu, M.; Poullain, G.; Raveau, B. *Physica C* **1992**, *198*, 193.

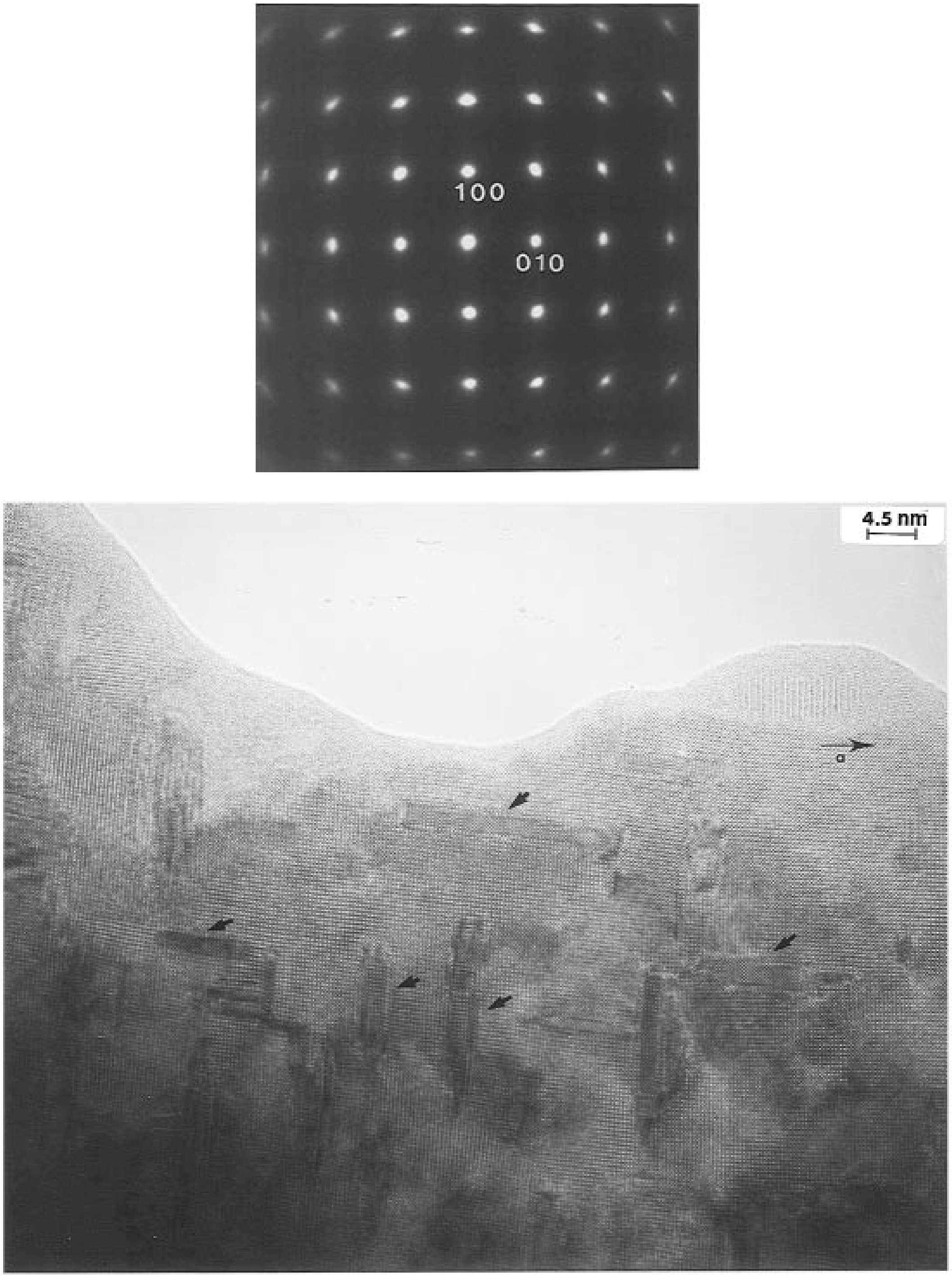

Figure 8. (a) ED of the film corresponding to the composition $Ba_2CaCu_2O_4CO_3$ taken along a direction perpendicular to the substrate and (b) corresponding overall HREM image.

is not the expected one, since the two structures do not exhibit a suitable orientation to build the accurate intergrowth. We indeed observed the formation of a patchwork of domains: [100] oriented $CaCuO_2$ domains in a [001] oriented $Ba_{2-x}Ca_xCuO_2CO_3$ matrix.

The stabilization of the member $Ba_{2-x}A_xCaCu_2O_4CO_3$ (A = Ca, Sr) using a multitarget system and starting from $Ba_{2-x}A_xCuO_2CO_3$ and $CaCuO_2$, is in progress.

No diamagnetic transition has been observed in any of these films down to 5 K. This point can be easily understood on the basis of charge balance considerations. The ideal composition $Ba_2CuO_2CO_3$ indeed involves only Cu^{2+}. The bulk oxycarbonate does not superconduct in the same way. The situation is different for the mixed Sr−Ba−Cu−C−O system, where superconductivity has been reported with a T_c (onset) of ≈40 K.[22] In fact, the actual composition of the material is $(Ba_{1-x}Sr_x)_2Cu_{1+y}O_{2+2y+z}(CO_3)_{1-y}$. The mixed valence of copper is then induced by the partial replacement of carbonate groups by copper polyhedra. Such compositions must be investigated for future thin films.

The original structural behavior of these materials confirms the interest of the replacement of copper polyhedra by CO_3 groups especially in the form of thin films. These results open the way to the synthesis of original phases using a multitarget system and confirm

---

(22) Kinoshita, K.; Yamada, T. *Nature* **1992**, *357*, 313.

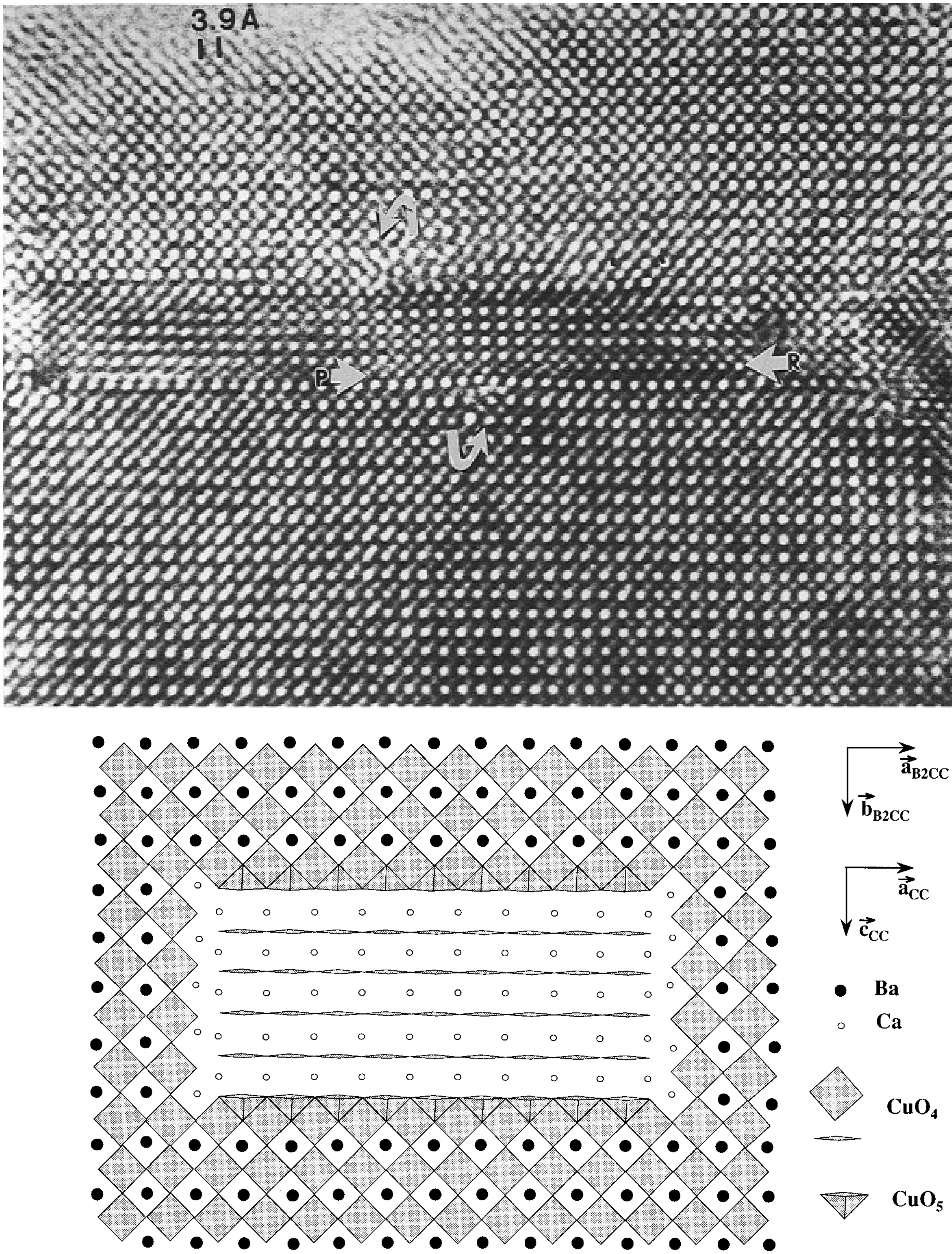

Figure 9. (a) Enlarged HREM image of the defects in $Ba_2CaCu_2O_4CO_3$ and (b) schematic model.

the difficulty to synthesize pure Ba−Ca−Cu−O oxycarbonates. These observations suggest the possibility to grow artificially the different member of the family $(CaCuO_2)_m(Ba_{2-x}A_xCuCO_3O_2)_n$ (A = Ca, Sr) and to induce superconductivity in this system.

Acknowledgment. The authors acknowledge financial support from the human capital and mobility EEC network "Chemical synthesis of novel superconductors".

CM9602508